Diamond & Related Materials 35 (2013) 36–39

Contents lists available at SciVerse ScienceDirect

Diamond & Related Materials

journal homepage: www.elsevier.com/locate/diamond

Strong photoluminescence from N-V and Si-V in nitrogen-doped ultrananocrystalline diamond film using plasma treatment

Tin Yu Ko [a], Yu Lin Liu [a], Kien Wen Sun [a,*], Yi Jie Lin [b], Shih-Chieh Fong [b], I Nan Lin [c], Nyan Hwa Tai [b]

[a] Department of Applied Chemistry, National Chiao Tung University, Hsinchu 30010, Taiwan
[b] Department of Materials Science and Engineering, National Tsing-Hua University, Hsinchu 300, Taiwan
[c] Department of Physics, Tamkang University, Tamsui 251, Taiwan

ARTICLE INFO

Article history:
Received 4 December 2012
Received in revised form 19 February 2013
Accepted 15 March 2013
Available online 26 March 2013

Keywords:
Ultrananocrystalline diamond
Nitrogen vacancy
Plasma
Photoluminescence
Color center

ABSTRACT

Raman, photoluminescence, and transport properties of nitrogen-doped ultrananocrystal diamond (UNCD) films were investigated following treatment with low energy microwave plasma at room temperature. The conductivity of nitrogen-doped UNCD films treated by microwave plasma was found to decrease slightly due to the reduced grain boundaries. We speculate that the plasma generated vacancies in UNCD films and provided heat for further mobilizing the vacancies to combine with the impurities, which led to the formation of the silicon-vacancy (Si-V) and nitrogen-vacancy (N-V) defect centers. The generated color centers were found to be distributed uniformly in the samples using a PL mapping technique. The PL emitted by the plasma treated nitrogen-doped UNCD film was strongly enhanced in comparison with the untreated films.

© 2013 Elsevier B.V. All rights reserved.

1. Introduction

The ultrananocrystalline diamond (UNCD) films grown from hydrogen-poor Ar/CH_4 microwave plasmas have attracted much attention as a promising material due to their unique and advantageous properties, including hardness, chemical inertness, high electron field emission [1,2], and possibility of n-type conductivities by doping [3]. Moreover, many physical properties, such as electrical conductivity [4], field emission threshold voltage [2], and mechanical [5] and optical properties [6], differ from other conventional diamond films.

However, up until now no evidence of nitrogen-related defects in UNCD films has been reported using luminescence spectroscopy. Nitrogen-doped UNCD thin films, which show lack of photoluminescence from typical N-V centers [7–10] found in diamond nanoparticles, indicate that most nitrogen, instead of being trapped as N-V complexes, is either incorporated as single substitutional atoms in the grains or in the amorphous carbon at the grain boundaries.

In recent years, in addition to quantum emitters, classical light sources based on luminescence from color centers in diamond have generated great interest for biomedical applications such as optical labels [11–13]. Nitrogen is the most prominently known impurity forming the nitrogen vacancy defect in diamond. The nitrogen vacancy defect in diamond consists of the substitution of nitrogen atom with the nearest vacancy. Two charge states of this nitrogen vacancy defect, neutral nitrogen vacancy center [$(N\text{-}V)^0$] and negatively-charged nitrogen vacancy center [$(N\text{-}V)^-$], are known from spectroscopic studies. [$(N\text{-}V)^0$] center has a nominal C_{3V} symmetry and zero-phonon E–A optical transition at 575 nm. The [$(N\text{-}V)^-$] center has been identified with a zero-phonon 637 nm corresponding to a ^3A-^3E transition and site symmetry C_{3V}. The model for neutral and negative charged N-V centers in diamonds has been fully discussed [7–10].

On the other hand, silicon vacancy center (Si-V) with a zero phonon emission and a phonon sideband at wavelengths of 738 nm and 757 nm, respectively, is another typical color center found in diamond [14,15]. In contrast to N-V center, Si atom enters the diamond lattice interstitially and then sits in the center of a split vacancy. Therefore, the Si-V center does not couple strongly with the diamond phonons, which results in a narrow emission spectrum with a sharp zero phonon line and a relatively weak phonon sideband. Si-V centers show a number of advantages in optical properties over N-V centers. For example, Si-V centers have a very weak vibronic sideband, which provides intense narrow-band emissions at room temperature as opposed to the broadband emission from N-V centers.

In earlier works, neutral vacancies were generated by high energy irradiation such as ion-beam or focused electron beam [16,17]. Subsequent to annealing at 700 °C, the vacancies became mobile. Some vacancies were trapped by substitutional nitrogen or silicon impurities and formed stable N-V or Si-V centers. In this report, we demonstrate a simple technique to generate efficient fluorescence defect centers in nitrogen-doped UNCD films at room temperature, which only requires low power and low energy microwave radiation.

* Corresponding author.
E-mail address: kwsun@mail.nctu.edu.tw (K.W. Sun).

0925-9635/$ – see front matter © 2013 Elsevier B.V. All rights reserved.
http://dx.doi.org/10.1016/j.diamond.2013.03.009

2. Sample preparation and characterization

Nitrogen-doped UNCD films were grown on SiO_2/Si substrates in microwave plasma enhanced chemical vapor deposition (MPECVD) system (IPLAS Cyrranus) with microwave power of 1400 W, pressure of 110 Torr, and substrate temperature of 800 °C for 45 min. Before the deposition, the substrates were seeded in an ultrasonic bath with nanodiamond particles from detonation synthesis (average size 4–6 nm). The Ar-rich mixture gases (73% Ar/25% N_2/2% CH_4) were used as the reaction gases during the growth. A thin layer of UNCD with a thickness of approximately 1 μm was formed on the template.

The high-resolution transmission electron microscope (HRTEM) images of the nitrogen-doped UNCD film indicate that the crystalline grain of the nanodiamond has a pin-like structure wrapped by the sp^2 C–C bondings. For low-nitrogen partial pressure the morphology of the films remains largely unchanged, with the grain size and grain boundary (GB) widths increasing only slightly. However, at high nitrogen partial pressure (> 10%), both the grain size and GB widths increase significantly [18–20]. The clustering of larger grains leads to the elongation of the nanocrystalline structures and eventually results in the formation of pin-like structures in the nitrogen-doped UNCD films.

Hall measurements made on the samples indicate that electrons are the majority carriers with a density of approximately 3.1×10^{20} cm^{-3} and a carrier mobility of 3.7 cm^2/Vs. The electrical conductivity is 138.29 Ω^{-1} cm^{-1} for the 25% nitrogen-doped UNCD film at room temperature based on the four-point-probe measurements. It has been proposed that the nearest-neighbor hopping or other thermally activated conduction mechanisms would occur in the GBs and result in greatly enhanced electron transport [4,21,22].

The Raman spectra for the undoped and nitrogen-doped UNCD films at the excitation wavelength of 488 nm are provided in Fig. 1. The Raman spectrum of the undoped UNCD film consists of five peaks, which indicates the characteristics of three different carbon phases: (1) diamond (at 1332 cm^{-1}), (2) amorphous sp^2 carbon (D-band at 1350 cm^{-1} and G-band at 1580 cm^{-1}), and (3) polyacetylene (at 1150 cm^{-1} and 1480 cm^{-1}) [23]. The increase of the amorphous sp^2 carbon and the reduction of the crystallinity as the nitrogen is introduced into UNCD film are clearly indicated by the disappearing of the diamond (1332 cm^{-1}) and polyacetylene peaks (1150 cm^{-1} and 1480 cm^{-1}) in the spectrum of the nitrogen-doped UNCD film. As shown in Fig. 3(b), the diamond peak becomes invisible on top of the D-band. The changes in relative intensity between D- and G-band and the shifting of the position of the G-band to higher wave numbers (from 1550 cm^{-1} to 1565 cm^{-1}) are clear indications of the noticeable changes in the content of the amorphous sp^2 carbon in the films [24].

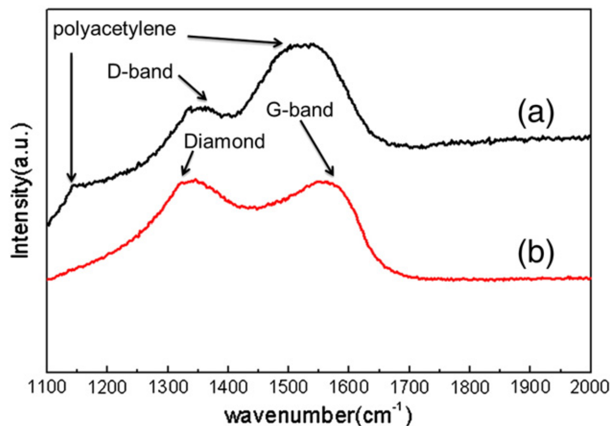

Fig. 1. Raman spectra of (a) undoped and (b) nitrogen-doped UNCD films.

3. Results and discussion

The nitrogen-doped UNCD film was treated by microwave plasma with a power of 800 W, total pressure 10 Torr, and at a substrate temperature of 300 K for 30 minutes. The simulated air (80% N_2/20% O_2) was used as the reaction gas during microwave plasma treatment. The HRTEM image of nitrogen-doped UNCD films shows that the morphology of the film remains unchanged and no re-growth is observed after the microwave treatment due to the low radiation power and energy. The conductivity of the nitrogen-doped UNCD film after microwave plasma treatment is only decreased slightly (dropped a fraction of 1 Ω^{-1} cm^{-1}). Judged by the evidence of reduction of sp^2 carbon phase in the Raman spectra, we attribute it to the slightly etching of the grain boundaries following treatment.

Fig. 2(a) and (b) show the Raman spectra of the nitrogen-doped UNCD films before and after the microwave plasma radiation. Following treatment, as shown in Fig. 2(b), the intensity of the Raman peaks from the amorphous carbon (D-band and G-band) is strongly attenuated due to the oxidation of the sp^2 carbon cluster by the oxygen in the reaction gases. Therefore, the peak of the diamond at 1332 cm^{-1} is clearly revealed. However, under high microwave power (>1400 W) and total pressure (~100 Torr), both the amorphous carbon and diamond become over etched and their corresponding Raman peak intensities are strongly attenuated, as shown in Fig. 2(c).

For the photoluminescence (PL) measurements, two nitrogen-doped UNCD samples, A and B, were fabricated under the same growth conditions except that sample B was intentionally positioned closer to the atomic gas of plasma during growth. Samples A and B before plasma treatment were both examined with an energy dispersive spectrometer (EDS) and secondary ion mass spectrometer (SMIS). The SIMS spectra are given in Fig. 3. In contrast to sample A, which contains only nitrogen impurities, sample B contains both the silicon and nitrogen impurities, as shown in Fig. 3. The gas sources used in the growth of nitrogen-doped UNCD films and the microwave plasma did not contain any silicon species. Therefore, the silicon impurities were introduced into sample B due to the etching of the silicon substrate with the sample positioned close to the atomic gas of plasma [25]. Although strong narrow-band luminescence from Si-V defects was observed in 5 nm crystallites of the UNCD film produced by the CVD technique [26]. However, in contrast to their results, our PL measurements showed no trace of N-V or Si-V related emission after etching away the amorphous carbon to completely exposed the embedded

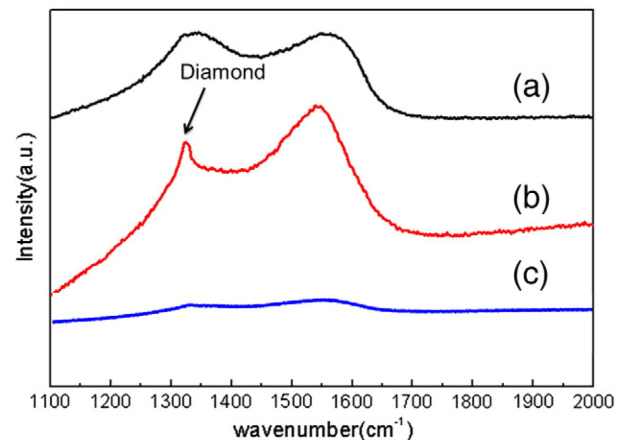

Fig. 2. Raman spectra of the nitrogen-doped UNCD films (a) before and (b) after microwave plasma with moderate power at room temperature. Spectrum of the sample after very intense microwave power (>1400 W) treatment at high pressure is displayed in (c).

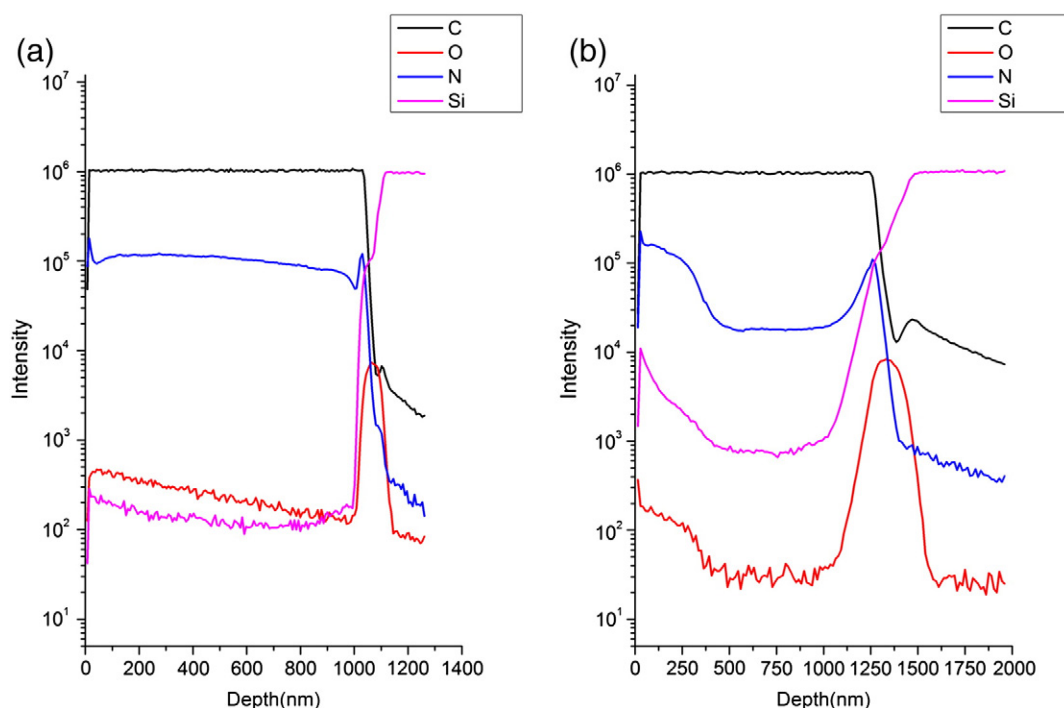

Fig. 3. Spectra from SIMS of (a) sample A and (b) sample B before plasma treatment.

crystalline nanodiamonds. It indicated that, after the film growth, no N-V or Si-V can be stably formed within the nanodiamond cores.

The PL spectra of samples A and B treated with microwave plasma are shown in Fig. 4. The spectrum of the sample without plasma treatment is also displayed in parallel for comparison. The two peaks at 522 nm and 528 nm are attributed to the Raman peaks of D-band and G-band. Although the EDS and SIMS spectra taken from inside the grains of samples A and B before plasma treatment show traces of nitrogen, samples without plasma treatment, however, show only a very weak or complete lack of photoluminescence from typical N-V centers found in the nanodiamonds [27]. On the contrary, the integrated PL intensity between 550 nm and 750 nm of plasma-treated samples A and B are greatly enhanced in compared to the untreated samples. In Fig. 4, the PL spectra between 550 nm and 750 nm can be fitted with two major peaks at 575 nm and 630 nm, respectively.

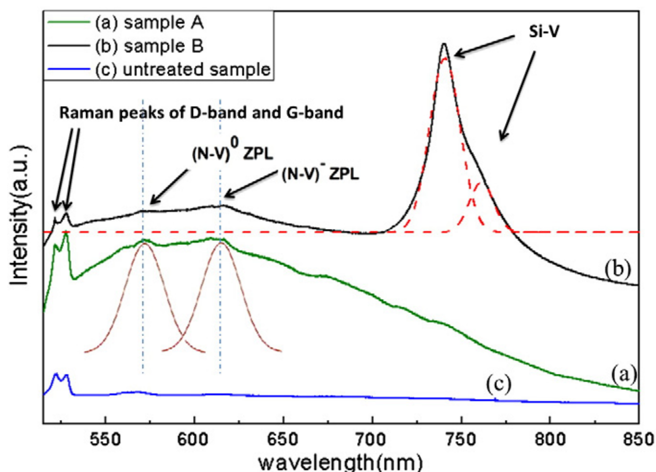

Fig. 4. Photoluminescence spectra of (a) sample A and (b) sample B following plasma treatment. Spectrum of the untreated sample is displayed in (c).

Therefore, the emissions between 550 nm and 750 nm are attributed to the $[(N\text{-}V)^0]$ and $[(N\text{-}V)^-]$ [7–10].

Two additional intense PL emissions at 738 nm and 757 nm are observed in sample B. By comparing the PL spectrum with earlier studies, we find that the additional peaks at 738 nm and 757 nm can be attributed to emission from Si-V. The PL spectrum reveals a very strong and sharp (FWHM of ~ 8 nm) zero phonon line on a weak background fluorescence and weak phonon side band (at ~ 755 nm). Similar result was also observed in bare nanodiamond particles of 500 nm and 6 nm average size seeded onto silicon templates and plasma treated using chemical vapor deposition [28]. It has been reported that the PL from Si-V was much stronger in synthetic diamonds with high concentration of nitrogen, but not in the nitrogen free diamond [14]. This is because the Si-V is normally in a more positively or neutrally charged state, which is not optically active. However, the isolated nitrogen atoms act as donors in diamond and pin the Fermi-level at approximately 1.7 eV below the conduction band. The number of Si-V in the optical inactive charged state is reduced with the higher position of the Fermi-level. Therefore, the emission from Si-V increases [28,29].

The in-depth distribution of generated fluorescent defect centers was found by the micro-PL mapping technology. First, we created a stepped slope along the surface of the nitrogen-doped UNCD film using a focus ion beam to expose the film at different depth. The scanning electron microscopy (SEM) image of the slope is provided in Fig. 5(a). The samples were scanned along a distance of 7 um with a step of 300 nm (indicated by the red line marked in Fig. 5(a)). The integrated PL intensities of Si-V (from 725 nm to 775 nm) and N-V (from 550 nm to 650 nm) as a function of the scanning distance are plotted in Fig. 5(b) and 5(c) at an excitation wavelength of 488 nm. The mapping results indicated that the integrated PL intensity varied linearly with the depth, which implies a uniform distribution of the N-V and Si-V defect centers inside the nitrogen-doped UNCD film. We speculated that the plasma generated vacancies in UNCD films and provided heat for further mobilizing the vacancies to combine with the impurities, which led to the formation of the silicon-vacancy (Si-V) and nitrogen-vacancy (N-V) defect centers. Due to

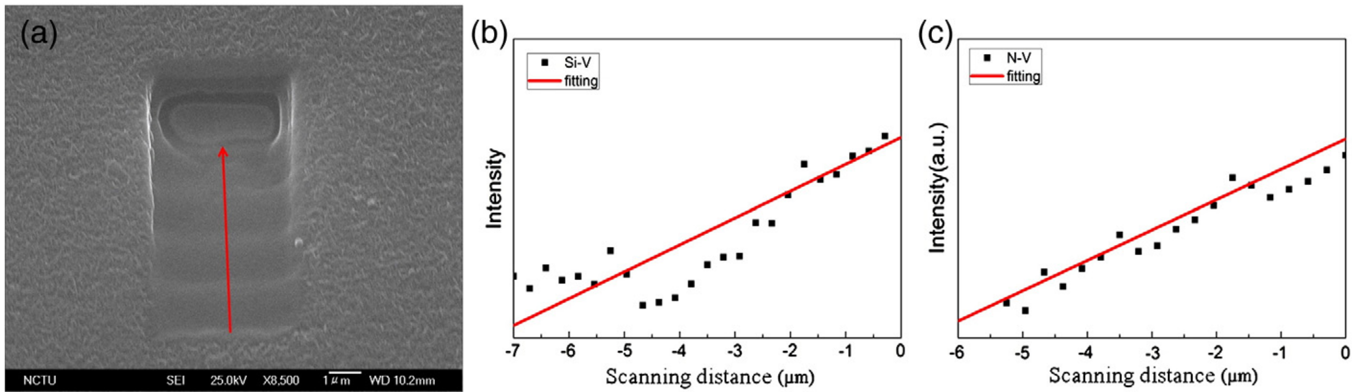

Fig. 5. (a) SEM image of the slope on the nitrogen-doped UNCD film. The integrated PL intensity from (b) Si-V (between 725 nm and 775 nm) and (c) N-V (between 550 nm and 650 nm) as a function of scanning distance.

the thickness of the film, the temperature profile created by the microwave absorption is rather uniform. Therefore, the vacancies can be uniformly driven throughout the film and form defect centers with the impurities.

4. Conclusion

In conclusion, we demonstrate a lower energy and low temperature technique to generate efficient fluorescence defect centers in nitrogen-doped UNCD films using microwave plasma. The intensity of Si-V emission can be further enhanced through controlled doping of nitrogen, which can reduce the population of the positively-charged/neutrally-charged optically-inactive Si-V state. In particular, the distributions of generated color centers, as ascribed to different vacancies, are spatially mapped and are shown to distribute uniformly in depth.

4.1. Diamond and related materials

4.1.1. Prime novelty statement

We demonstrate a lower power and lower temperature means of generating intense photoluminescence in nitrogen-doped UNCD films using microwave plasma. The PL mapping results show that the plasma generated N-V is uniformly distributed in the nitrogen-doped UNCD film.

Acknowledgements

The current work was supported by the National Science Council of the Republic of China under Grant No. NSC 99-2119-M-009-004-MY3 and the MOE ATU program.

References

[1] D. Zhou, A.R. Krauss, L.C. Qin, T.G. McCauley, D.M. Gruen, T.D. Corrigan, R.P.H. Chang, H. Gnaser, J. Appl. Phys. 82 (1997) 4546–4550.
[2] A.R. Krauss, O. Auciello, M.Q. Ding, D.M. Gruen, Y. Huang, V.V. Zhirnov, E.I. Givargizov, A. Breskin, R. Chechen, E. Shefer, V. Konov, S. Pimenov, A. Karabutov, A. Rakhimov, N. Suetin, J. Appl. Phys. 89 (2001) 2958–2967.
[3] O.A. Williams, S. Curat, J.E. Gerbi, D.M. Gruen, R.B. Jackman, Appl. Phys. Lett. 85 (2004) 1680–1682.
[4] S. Bhattacharyya, O. Auciello, J. Birrell, J.A. Carlisle, L.A. Curtiss, A.N. Goyette, D.M. Gruen, A.R. Krauss, J. Schlueter, A. Sumant, P. Zapol, Appl. Phys. Lett. 79 (2001) 1143–1441.
[5] C. Zuiker, A.R. Krauss, D.M. Gruen, X. Pan, J.C. Li, R. Csencsits, A. Erdemir, C. Bindal, G. Fenske, Thin Solid Films 270 (1995) 154–159.
[6] T. Sharda, M.M. Rahaman, Y. Nukaya, T. Soga, T. Jimbo, M. Umeno, Diamond Relat. Mater. 10 (2001) 561–567.
[7] Y. Mita, Phys. Rev. B 53 (1996) 11360–11364.
[8] G. Davies, M.F. Hamer, Series A, Mathematical and Physical Sciences, 348, 1976, pp. 285–298.
[9] G. Davies, S. Lawson, A. Collins, A. Mainwood, S. Sharp Physical, Review B 46 (1992) 13157–13170.
[10] G. Davies, Nature 269 (1977) 498–500.
[11] J. Chao, E. Perevedentseva, P. Chung, K. Liu, C. Cheng, C. Chang, Biophysical Journal 93 (2007) 2199–2208.
[12] O. Faklaris, V. Joshi, T. Irinopoulou, P. Tauc, M. Sennour, H. Girard, C. Gesset, J.-C. Arnault, A. Thorel, J.-P. Boudou, P.A. Curmi, F. Treussart, ACS Nano. 3 (2009) 3955–3962.
[13] S.J. Yu, M.W. Kang, H.C. Chang, K.M. Chen, Y.C. Yu, J. Am. Chem. Soc. 127 (2005) 17604–17605.
[14] A.T. Collins, M. Kamo, Y. Sato, J. Mater. Res. 5 (1990) 2507–2514.
[15] J. Ruan, W.J. Choyke, W.D. Partlow, Appl. Phys. Letts. 58 (1991) 295–297.
[16] S.D. Wolter, M.T. Mcclure, J.T. Glass, B.R. Stoner, Appl. Phys. Letts 66 (1995) 2810–2812.
[17] J.K. Yan, L. Chang, Nanotechnology 17 (2006) 5544–5548.
[18] D.M. Gruen, P.C. Redfern, D.A. Horner, P. Zapol, L.A. Curtiss, J. Phys. Chem. B 103 (1999) 5459–5467.
[19] P. Zapol, M. Sternberg, L. Curtiss, T. Frauenheim, D. Gruen, Physical Review B 65 (2001) 045403.1–045403.11.
[20] J. Birrell, J.A. Carlisle, O. Auciello, D.M. Gruen, J.M. Gibson, Appl. Phys. Letts. 81 (2002) 2235–2237.
[21] S. Bhattacharyya, Phys. Rev. B 70 (2004) 125412-1-125412-10.
[22] K. Shah, D. Churochkin, Z. Chiguvare, S. Bhattacharyya, Physical Review B 82 (2010) 184206-1-184206-9.
[23] I.I. Vlasov, V.G. Ralchenko, E. Goovaerts, A.V. Saveliev, M.V. Kanzyuba, Phys. Status Solidi 203 (2006) 3028–3035.
[24] I.I. Vlasov, E. Goovaerts, V.G. Ralchenko, V.I. Konov, A.V. Khomich, M.V. Kanzyuba Diamond, Diamond Relat. Mater. 16 (2007) 2074–2077.
[25] I.I. Vlasov, V.G. Ralchenko Defect, Diffus. Forum 226–228 (2004) 61–65.
[26] I.I. Vlasov, A.S. Barnard, V.G. Ralchenko, O.I. Lebedev, M.V. Kanzyuba, A.V. Saveliev, V.I. Konov, E. Goovaerts, Adv. Mater. 21 (2009) 808–812.
[27] Y.L. Liu, K.W. Sun, Appl. Phys. Letts. 98 (2011) 153702.
[28] S.A. Catledge, S. Singh, Adv. Sci. Lett. 4 (2011) 512.
[29] S. Singh, S.A. Catledge, J. Appl. Phys. 113 (2013) 044701.